

An Investigation of Critical Issues in Bias Mitigation Techniques

Robik Shrestha¹ Kushal Kafle² Christopher Kanan^{1,3,4}

¹Rochester Institute of Technology ²Adobe Research ³Paige ⁴Cornell Tech

¹{rss9369, kanan}@rit.edu ²{kkafle}@adobe.com

Abstract

A critical problem in deep learning is that systems learn inappropriate biases, resulting in their inability to perform well on minority groups. This has led to the creation of multiple algorithms that endeavor to mitigate bias. However, it is not clear how effective these methods are. This is because study protocols differ among papers, systems are tested on datasets that fail to test many forms of bias, and systems have access to hidden knowledge or are tuned specifically to the test set. To address this, we introduce an improved evaluation protocol, sensible metrics, and a new dataset, which enables us to ask and answer critical questions about bias mitigation algorithms. We evaluate seven state-of-the-art algorithms using the same network architecture and hyperparameter selection policy across three benchmark datasets. We introduce a new dataset called *Biased MNIST* that enables assessment of robustness to multiple bias sources. We use *Biased MNIST* and a visual question answering (VQA) benchmark to assess robustness to hidden biases. Rather than only tuning to the test set distribution, we study robustness across different tuning distributions, which is critical because for many applications the test distribution may not be known during development. We find that algorithms exploit hidden biases, are unable to scale to multiple forms of bias, and are highly sensitive to the choice of tuning set. Based on our findings, we implore the community to adopt more rigorous assessment of future bias mitigation methods. All data, code, and results are publicly available¹.

1. Introduction

Deep learning systems are trained to minimize their loss on a training dataset. However, datasets often contain spurious correlations and hidden biases which result in systems that have low loss on the training data distribution, but then fail to work appropriately on minority groups because they exploit and even amplify these spurious correlations [71, 36]. For example, in systems trained to infer hair color on the

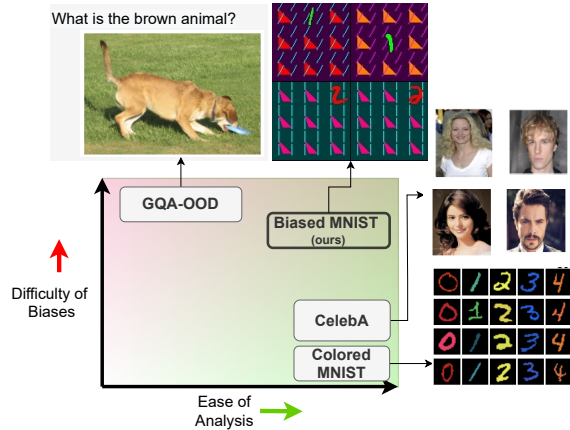


Figure 1: Current bias mitigation systems are tested on simple datasets that are easy to analyze, but do not offer challenges present in realistic cases. Addressing this, we propose the *Biased MNIST* dataset which is easy to analyze, yet is reflective of real world challenges since it contains multiple sources of biases. We also test on GQA-OOD, where the sources of biases are not very obvious.

CelebA dataset [43], the majority group of non-blond males occurs 50 times more than the minority group of blond males, resulting in systems incorrectly predicting non-blond as hair color for the minority group. While this is a toy problem, in the real world, hidden minority patterns are common and failing on them can have dire consequences. Systems designed to aid human resources, help with medical diagnosis, determine probation, or loan qualification could be biased against minority groups based on age, gender, religion, sexual orientation, ethnicity, or race [54, 8, 17, 14, 48]. Systems can exploit correlated variables even if they are not directly a part of the input e.g., through inferred zip codes [22], failing to work effectively on minority groups.

Recently, many methods have been proposed to make neural networks bias resistant. These methods can be grouped into two types: 1) those that assume the bias variables e.g., the gender label in CelebA, are explicitly annotated and can be accessed during training [55, 55, 69, 38] and, 2) those that do not require explicit access [46, 50]. Assuming explicit access requires extra annotations in addition to the

¹<https://github.com/erobic/bias-mitigators>

actual target, and for many tasks it may not be immediately clear what the bias variables are e.g., biases may only be discovered years later [51, 50]. Methods that do not assume access to these bias variables have only recently been proposed [46, 65, 50].

So far, there is no study comparing methods from either group comprehensively. Often papers fail to compare against recent methods and vary widely in the protocols, datasets, architectures, and optimizers used. For instance, the widely used Colored MNIST dataset, where colors and digits are spuriously correlated with each other, is setup differently across papers. Some use it as a binary classification task (class 0: digits 0-4, class 1: digits: 5-9) [5, 50], whereas others use a multi-class setting (10 classes) [38, 41]. For CelebA, [46] uses ResNet-18 whereas [50] uses ResNet-50, but the comparison was done without taking this architectural change into account. These discrepancies make it difficult to judge the methods on an even ground.

Methods are typically highly sensitive to hyperparameter choices, and papers report numbers on systems in which the hyperparameters were tuned using the test set distribution [19, 50, 64]. In the real world, biases may stem from multiple factors and may change in different environments, making this setup unrealistic. Furthermore, tuning on the test distribution can lead to methods that are right for the wrong reasons. When this is done, systems can perform well just by exploiting the biases they are supposed to overcome [62, 64], and they will then fail once deployed because they have not really learned to solve the task.

In addition, we posit that the commonly used benchmarks are not challenging enough to test generalization to realistic scenarios. For example CelebA and Colored MNIST, two of the most widely used benchmarks, contain a single bias variable to mitigate: gender and color respectively. It is unclear how well methods would fare in presence of multiple types of bias, e.g., position or co-occurring objects/patterns, which are commonly present in real-world datasets. For some tasks it can be impossible to exhaustively enumerate all bias variables. For example, in visual question answering (VQA), where a system answers questions about images, biases can stem from: object-context co-occurrences, visual concept/language correlations, question type/answer distributions, and more. For explicit bias mitigation methods, it is unclear what kinds of annotations are required to address all of these biases. Even when some annotations are provided, these may entail generalization to thousands of groups. For instance, answering questions about ‘bags’, while remaining robust to explicitly specified correlations with object category/attributes can lead to numerous groups: ‘red bags’, ‘blue bags’, ‘leather bags’, ‘plastic bags on a shelf’ etc. It is unknown if methods work well at such scales.

We address the above issues via these contributions:

1. We describe our new Biased MNIST dataset and corresponding evaluation protocol for measuring resistance to multiple forms of bias. It measures resistance to spuriously correlated background/foreground color, texture, co-occurring distractors, position, and more.
2. We compare seven state-of-the-art bias mitigation methods on classification tasks using Biased MNIST and CelebA, measuring generalization to minority patterns, scalability to multiple sources of biases, sensitivity to hyperparameters, etc. We ensure fair comparisons by using the same architecture, optimizer, and performing grid searches for hyperparameters.
3. To go beyond image classification, we measure the performance of these methods on the biased GQA benchmark for VQA.
4. We provide concrete recommendations for future studies, so that comparisons among algorithms are meaningful and reflective of real-world challenges.

2. Bias and Bias Resistance Metrics

We study bias in supervised classification. To properly study bias mitigation, it is necessary to provide a definition of biased data and biased behavior in a model. We wish to learn a function $f : X \rightarrow Y$ which outputs a categorical target $y \in Y$ given $x \in X$. Each x is itself a mixture of a signal s that we wish the system to use for inference and bias b that is spuriously correlated with y , but we want the system to be invariant to it. The spurious correlations between y and b do not always hold, so if a system uses b to infer y , it will not generalize. However, rather than becoming invariant to the bias variables, systems often exploit them, especially when they are easier to learn than the signal [50, 59].

Bias resistance can be measured by intentionally introducing covariate shift e.g., with a test dataset distribution that differs from training or a metric that balances performance across groups. While this can also be used to study the cross-domain setting which entails generalization to new sources of bias or data domains that are not present in the training set [10], our study focuses on the cross-bias setting defined by [6], where the same set of bias variables are present in both train and test sets.

We will now describe how y and b can be used to divide the dataset into different groups and then present metrics that use the groups to measure bias resistance. Let us consider b to be comprised of $|b|$ bias variables: $b = \{b_1, b_2, \dots, b_{|b|}\}$. We consider every unique combination of b and y to be a different group g . For instance, $b_1 = \text{gender} \in \{\text{Male}, \text{Non-Male}\}$ and $y \in \{\text{Blond}, \text{Non-Blond}\}$ result in four groups for CelebA.

Metrics. We first define an accuracy metric (Acc) that can interpolate within as well as extrapolate beyond the train

and test distributions:

$$Acc(\alpha) = \frac{\sum_{g=1}^{|G|} p_g^\alpha Acc_g}{\sum_{g=1}^{|G|} p_g^\alpha},$$

where, p_g denotes the train prior for group g , $|G|$ is the total number of groups and α is used to shift the prior. When $\alpha = 0$, $Acc(\alpha = 0)$ yields the mean per group accuracy (MPG) or **unbiased accuracy**, whereas when $\alpha = 1$, then weights reflect the train priors/biases. When $0 < \alpha < 1$, it interpolates between biased (train) priors and unbiased group weights. When $\alpha < 0$, minority groups are weighed more and when $\alpha > 1$, majority groups are weighed more i.e., it amplifies the train bias. Unless otherwise specified, we treat $Acc(\alpha = 0)$, i.e., unbiased accuracy as our target metric since it weighs all groups equally.

We define two more metrics to help measure bias resistance. **Majority/Minority Difference (MMD)** simply measures the difference between majority and minority groups:

$$MMD = [Acc_{majority} - Acc_{minority}].$$

High MMD indicates that methods rely on factors that work for majority groups, but not for minority groups. The second metric is **Improvement Over the Standard Model (IOSM)**, which measures the difference in group g 's accuracy as compared to the standard model (StdM) i.e.,

$$IOSM_g = [Acc_g - Acc_{StdM,g}].$$

Ideal method would obtain high $IOSM_g$ across all groups.

3. Bias Mitigation Strategies

Without bias mitigation mechanisms, **standard models (StdM)** often use spurious bias variables for inference, rather than developing invariance to them, which often results in their inability to perform well on minority patterns [28, 12, 3, 61]. To address this, several bias mitigation mechanisms have been proposed, and they can be categorized into two groups: 1) methods that access explicit bias labels during training, and 2) methods that do not assume such access. We briefly review methods from these categories, with an emphasis on the methods assessed in our studies.

3.1. Explicit Bias Mitigation Methods

Explicit bias mitigation techniques directly access the bias variables: $b_{expl.}$ during training to develop invariance to them. Based on the way these variables are utilized during training, we choose five different explicit methods for our study. We refer to them as **explicit methods** for conciseness.

Re-sampling/Re-weighting: These approaches attempt to learn invariances by balancing out the spurious correlations. The classical approach is to re-balance the class distribution by adjusting the sampling probability/ loss weight for

majority/minority samples [15, 27, 42, 72, 21]. This includes synthesizing minority instances too [15, 27]. Moving beyond class imbalances, REPAIR [41] proposed learning dynamic weights to mitigate representation bias [40]. However, [55] have shown promising results by using static weights to up-weight minority patterns. We choose this method due to its simplicity.

Group Upweighting (Up Wt) [55] attempts to mitigate the correlations between y and $b_{expl.}$ by upweighting the minority patterns. Specifically, each sample (x, y) is assigned to a group: $g = (y, b_1, b_2, \dots, |b_{expl.}|)$, and the loss is scaled by $\frac{1}{N_g}$, where N_g is the number of instances in group g . Up Wt requires the models to be sufficiently regularized, i.e., be trained with low learning rates and/or high weight decays to be robust to the minority groups.

Distributionally Robust Optimization (DRO): DRO [23] minimizes the worst-case expected loss over potential test distributions. Often, such distributions are approximated by sampling from a uniform divergence ball around the train distribution [11, 24, 47]. However, this lacks structured priors about the potential shifts, and instead hurts generalization [33].

Group DRO (GDRO) [55] provides DRO with the necessary prior that it must generalize to all groups. Similar to Up Wt, GDRO also uses y and $b_{expl.}$ to create groups and has been shown to work well with sufficiently regularized models. However, unlike Up Wt, it performs weighted sampling from each group and has an optimization procedure to minimize the loss over the worst-case group.

Ensembling Approaches: Ensembling approaches [29, 18, 13] have a two-branch setup: a) a bias-only branch f_b that predicts y from b alone to identify the bias-prone samples, and b) a de-biased branch $f_d(\cdot)$ that is trained to focus on samples that f_b finds difficult so that it learns richer features that work on difficult samples too. The two branches can be ensembled in different ways. DRiFt [29] uses product-of-experts [32] and LearnedMixin [18] extends this through learned weights and entropy constraints that control f_b .

Reduction of Unimodal Biases (RUBi) [13] multiplies the outputs from $f_d(\cdot)$ with sigmoided outputs from $f_b(\cdot)$, thereby assigning higher loss weights to samples that cannot be predicted through biases alone. RUBi was the previous state-of-the-art on VQA-CP [3], a testbed for measuring robustness to biases in VQA. For the bimodal problem of VQA, the original implementation focused on linguistic biases, training f_b on question features only. For our studies, we instead train f_b on $b_{expl.}$ directly, to control the type of biases captured by f_b . We assess RUBi [13] over others since it performed better in the preliminary studies.

Adversarial Debiasing: These techniques impair the ability of the representation learner to encode biases [69, 1, 52, 26]. Like ensembling methods, they also employ a two-branch setup, with the representation encoder in the

main branch being penalized if the bias-only branch: $f_b()$ is successful at predicting biases from them [69]. Alternately, $f_b()$ may be trained to predict the class label from the biased features [52, 26], but in either case, the gradient from $f_b()$ is reversed during backpropagation for debiasing.

Learning Not to Learn (LNL) [38] uses an adversarial setup derived from minimization of mutual information between representation and bias. In addition to the gradient reversal, the mutual information formulation introduces an entropy regularization on the bias predictions.

Invariant Risk Minimization (IRM): The goal of IRM is to extract representations that are invariant across environments: $\mathcal{E} = \{e_1, e_2, \dots, e_E\}$, each encoding different spurious correlations [5, 63, 16]. Such representations enable the same classifier to be simultaneously optimal over all \mathcal{E} . For this, [5] propose to regularize the gradient norm of a fixed linear classifier. More recent variants include regularization of variance of risks [39, 67]. However, [53] have shown that such objectives can fail to recover the invariant features in practice. Despite this negative result, we still compare against IRM since it is a promising research direction.

IRMv1 [5] is an efficient approximation of an otherwise computationally expensive bi-level IRM objective. It consists of a regularization constraint on the gradient norm with respect to a fixed scalar $\theta_c = 1.0$:

$$\min_{\theta} \sum_{e \in \mathcal{E}_{tr}} l^e(\hat{y}) + \lambda \|\nabla_{\theta_c|_{\theta_c=1.0}} l^e(\theta_c \cdot \hat{y})\|^2,$$

where, l^e is loss on environment e , \hat{y} is the logit vector yielded by the model parameterized by θ and λ balances between the empirical risk and invariance. In our experiments, we use the previously defined explicit data groups as the training environments for IRM.

3.2. Implicit Bias Mitigation Methods

Since explicit access to bias variables is an undesirable requirement in practice, some recent methods have proposed to mitigate biases without such assumptions. We call them **implicit methods** for conciseness and describe them below.

Limited Capacity Models: Most implicit methods assume that easy-to-learn biases can be captured by limiting the capacity of the models [65, 57, 46]. The capacity of such bias-prone models: $f_b()$ can be limited by using a small subset of train instances for a few epochs [65], using fewer model parameters [57], attaching a classifier to intermediate layers, instead of using the final representation layers [19], using bias-prone architectures [7] or amplifying biases [46]. Main network: f_d is then debiased by assigning higher weights to the harder samples, so that it generalizes to samples that cannot be predicted through biases alone.

Learning From Failure (LFF) [46] amplifies the bias in

f_b using the generalized cross entropy loss [70]:

$$GCE(s(x; \theta), y) = \frac{1 - s_y(x; \theta)^\gamma}{\gamma},$$

where s_y is the softmax score for the ground truth class and γ determines the degree of bias amplification. Samples with high f_b loss are then assigned higher weights while training f_d . While γ seems critical, the original paper does not discuss a way to tune it and instead fixes it to a default value of $\gamma = 0.7$. In fact, the paper does not provide details on model selection at all; however, this is an important question, which we discuss in Sec. 6.4.

Gradient Starvation Mitigation: Different from the limited capacity methods, spectral decoupling [50] aims to overcome the issue of gradient starvation [20], which is the tendency to only rely on statistically dominant features. This is related to the simplicity bias exploitation, where models exploit the simplest features despite having access to more predictive features [59, 31], which are more complex.

Spectral Decoupling (SD) [50] aims to decouple the learning dynamics between features. The authors show that regularizing the network outputs (\hat{y}) as:

$$\frac{\lambda}{2} \|\hat{y} - \gamma\|_2^2,$$

where, λ and γ are hyperparameters, provably decouples the learning dynamics, enabling learning of better features.

4. Datasets

We use datasets that enable probing existing methods with critical questions regarding their robustness. We test on datasets with varying scales and types of biases, allowing us to perform highly controlled studies that analyze scalability to a large number of hidden groups.

4.1. Biased MNIST

Existing datasets for assessing bias mitigation methods do not enable analysis of multiple bias sources, e.g., Colored MNIST only tests for color versus class bias. To address this, we created the Biased MNIST dataset, which consists of 3×3 grids, where the task is to recognize the digit (0 – 9) placed at a particular cell in the grid while being robust to multiple sources of biases (see Fig. 2). These biases include: a) background color, b) color of the target digit, c) position of the digit (among 9 grid locations), d) distractor shapes, which are placed on all cells except the cell with the digit, e) color of the distractors, f) type of texture, and g) texture color. Each digit co-occurs more frequently with a particular value for each bias type e.g., digit ‘1’ is usually green, placed on a purple background and co-occurs mainly with right-angled triangles as distractors. Formally, b_j represents the j^{th} bias type e.g., $b_1 =$ background color. Each b_j can take one of

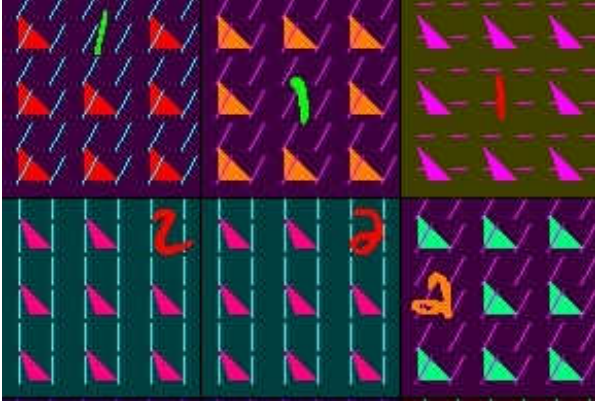


Figure 2: Biased MNIST requires the methods to classify the target digit while remaining invariant to biases.

10 discrete values, with k^{th} value being denoted by: $b_{j,k}$ e.g., 9^{th} background color is $b_{1,9} = \text{blue}$. The biases are conditionally independent from each other and dependent only on the digit. That is, each digit d_i co-occurs with its biased value: b_{ji} for b_j with probability: $p(b_{ji}|d_i)$, otherwise co-occurs with one of the remaining values with uniform probability: for $l \neq i$, $p(b_{jl}|d_i) = \frac{1-p(b_{ji}|d_i)}{9}$. Unless otherwise specified, we set $p(b_{ji}) = p_{\text{bias}} = 0.7$ in the train set, while testing on an unbiased test set with $p_{\text{bias}} = 0.1$. This setup allows us to study multiple sources of biases and scalability to large number of majority/minority groups.

4.2. CelebA

The CelebA dataset [43] of celebrity faces is widely used to assess bias mitigation techniques [55, 56, 46, 50]. Following earlier work, it is used for binary hair color classification (blond or non-blond), which is correlated with gender. There are two major bias sources: a) class imbalance, with non-blond occurring 5.7 times more than blond hair color, and b) presence of a rare group, i.e., blond male celebrities only account for 0.86% of the training instances.

4.3. GQA-OOD

We use the GQA visual question answering dataset [34] to highlight the challenges of using bias mitigation methods on real-world tasks. It has multiple sources of biases including imbalances in answer distribution, visual concept co-occurrences, question word correlations, and question type/answer distribution. It is unclear how the explicit bias variables should be defined so that the methods can generalize to all minority groups. GQA-OOD [37] divides the evaluation and test sets into majority (head) and minority (tail) groups based on the answer frequency within each ‘local group’ (e.g., colors of bags), which is a unique combination of answer type (e.g., colors) and the main concept (e.g., ‘bag’, ‘chair’, etc.). The head/tail categorization makes

analysis easier; however, it is unclear how one should specify the explicit biases so that the models generalize even to the rarest of local groups. Therefore, we explore multiple ways of defining the explicit bias variable in separate experiments: a) majority/minority group label (2 groups), b) answer class (1833 groups), c) global group (115 groups) and d) local group (133328 groups). It is unknown if bias mitigation methods can scale to hundreds and thousands of groups in GQA, yet natural tasks require such an ability.

5. Network Architecture & Tuning Procedure

For each dataset, we assess all bias mitigation methods with the same neural network architecture. For CelebA, we use ResNet-18 [30]. For Biased MNIST, we use a convolutional neural network with four ReLU layers consisting of a max pooling layer attached after the first convolutional layer. For GQA-OOD, we employ the UpDn architecture [4], which is widely used for VQA [58, 37, 66].

For each dataset, we use the class label y and the explicit bias variables b_{expl} to define explicit groups for Up Wt, GDRO and IRMv1. For instance, for CelebA, hair color and gender result in four explicit groups while for Biased MNIST, the number of groups: $|G|$ depends on the number of explicit bias variables: $|b_{\text{expl}}|$, with $|G| = 10^{|b_{\text{expl}}|}$. We will specify the exact b_{expl} for each experiment in Sec. 6. For GQA, we use head/tail, answer class, global and local groups as explicit variables. For all datasets, RUBi uses b_{expl} to predict y , whereas LNL trains the adversarial branch to predict b_{expl} from representations. Of course the implicit methods: StdM, LFF and SD are invariant to the choice of the explicit biases during training. Unless otherwise specified, results from Biased MNIST are averaged across 3 random seeds, but due to computational constraints, we ran models on CelebA and GQA-OOD only once.

Hyperparameters for each method were chosen using a grid search with unbiased accuracy on each dataset’s validation set. To make this tractable, we first ran a grid search for the learning rate over $\{10^{-3}, 10^{-4}, 10^{-5}\}$ and weight decay over $\{0.1, 10^{-3}, 10^{-5}, 0\}$. After the best values were chosen, we searched for method-specific hyperparameters. Due to the size of GQA-OOD, hyperparameter search was performed by training on only 10% of instances, and then the best selected hyperparameters were used with the full training dataset. The exact values for the hyperparameters are specified in the Appendix.

6. Questions Posed and Answered

In this section, we probe the existing methods with critical questions regarding their robustness, meanwhile proposing metrics and empirical setups to study them. We first describe the metrics and then present the results.

Table 1: Unbiased accuracies $Acc(\alpha = 0)$ on all datasets for all methods. We format the *first*, *second* and *third* best results. Methods that do not access explicit biases have gray background.

Methods/ Datasets	CelebA	Biased MNIST	GQA
StdM	80.3	42.0	44.8
Up Wt [56]	87.4	30.1	30.0
GDRO [55]	88.5	27.2	26.4
RUBi [13]	87.2	38.9	24.1
LNL [38]	79.2	40.6	28.6
IRMv1 [5]	79.8	38.7	39.3
LFF [46]	77.8	<u>56.6</u>	45.1
SD [50]	<u>88.6</u>	<u>41.3</u>	<u>46.9</u>

6.1. Head-to-Head Comparisons

Question 1: Are there clear winners in a head-to-head comparisons across datasets?

We first compute the unbiased accuracies for all eight methods on all three datasets in Table. 1. We first train explicit methods on CelebA, using class and gender labels as explicit biases. For Biased MNIST, there are multiple ways to define explicit biases, but for this section, we simply use each of the seven variables as explicit biases in different runs and average across the runs. We study combinations of multiple explicit variables in Sec. 6.3. We set $p_{bias} = 0.7$ for this section, and present results across different p_{bias} in the Appendix. Similarly for GQA, we consider each of the four variables as explicit bias in separate runs and present the average.

Results. As shown in Table. 1, no method performs universally well across datasets; however, the implicit methods LFF and SD obtain high unbiased accuracies on most datasets. This shows that implicit methods can deal with multiple bias sources without explicit access. Explicit methods work well on CelebA but fail on Biased MNIST and GQA. Specifically, Up Wt, GDRO and RUBi obtain 7-8% improvements over StdM on CelebA, which requires generalization to only 4 groups. However, all explicit methods perform worse than StdM on Biased MNIST and GQA, signifying their inability to deal with multiple bias sources. LNL and IRMv1 were comparable to StdM even on CelebA, demonstrating lack of generalization even on simple settings. Despite being a simpler method, Up Wt outperformed GDRO on both Biased MNIST and GQA, but both were worse than StdM. These results show that implicit methods can outperform explicit methods.

6.2. Bias Exploitation

Question 2: Do methods show robustness to both explicit and implicit biases?

In this set of experiments, we study the exploitation of

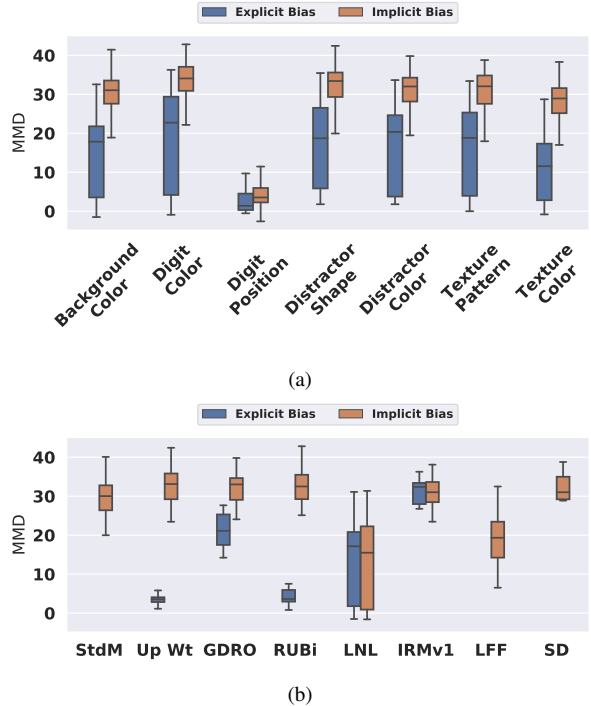


Figure 3: Boxplots of differences between majority and minority groups (MMD) on Biased MNIST over: a) bias variables and b) different methods.

explicit and implicit bias. We primarily focus on the Biased MNIST dataset. Specifically, we reserve each individual variable as the explicit bias in separate experiments, while treating the remaining six as implicit biases. As shown in Fig. 3, the majority minority differences (MMD) across explicit and implicit biases help us diagnose bias exploitation. We also analyze per-group accuracies on CelebA, to examine behavior in a simpler setting.

Results. As shown in Fig. 3a, we find that methods tend to latch onto all sources of implicit bias, with the exception of digit position. As shown in Fig. 3b, some explicit methods attempt to mitigate the explicit bias to an extent, with Up Wt, GDRO and RUBi obtaining lower MMD values for explicit variables in comparison to implicit variables. However, despite the decrease in MMD for explicit variables, the poor results in Table. 1 and high MMD values for implicit variables in Fig. 3a suggest that the overall generalization is still worsened due to implicit biases. We explore if explicit methods generalize if all bias sources are explicitly specified in Sec. 6.3. Among the implicit methods, LFF, which obtained the best unbiased accuracy on Biased MNIST also shows the lowest MMD, further indicating its ability to deal with multiple sources of bias. Also, we observe large inconsistencies in the variables exploited across the methods. Even different runs of the same method with the same hyperparameters

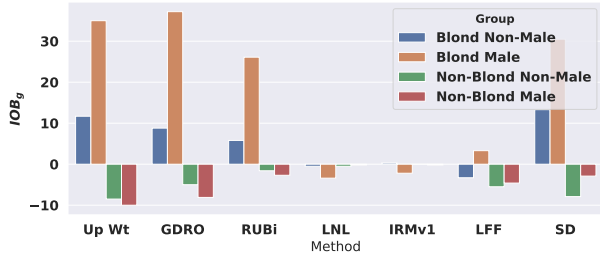


Figure 4: Improvement Over the Standard Model (IOSM) for each group of CelebA.

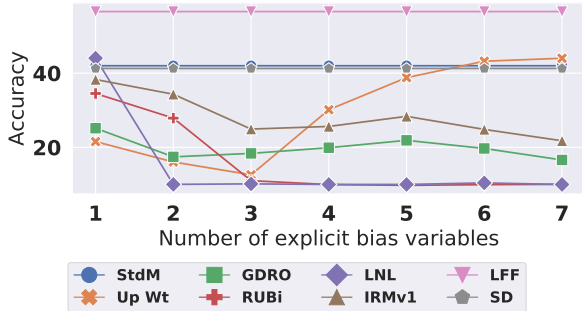


Figure 5: Unbiased accuracy as a function of number of explicit bias variables. StdM, LFF and SD are invariant to the choice of explicit bias variables.

result in exploitation of different biases. We hypothesize that all of these variables offer plausible prediction rules for the models to latch onto, and the initial randomness drives the methods towards exploiting one variable over the others.

Finally, we study the per-group accuracies in CelebA using the *IOSM* plot in Fig. 4. The improvements in blond (minority class) incur degradation in non-blond (majority class). The methods tilt predictions either in the favor of minority or majority classes, which further reflects the inability to learn the signal even in simple settings.

6.3. Scalability of Methods

Question 3: Do methods scale up to multiple types of biases and a large number of dataset groups?

It is unknown how well the methods scale up to multiple sources of biases and large number of groups, even when they are explicitly annotated. To study this, we train the explicit methods with multiple explicit variables for Biased MNIST and individual variables that lead to hundreds and thousands of groups for GQA and compare them with the implicit methods. For Biased MNIST, we first sort the seven total variables in the descending order of MMD (obtained by StdM) and then conduct a series of experiments. In the first experiment, the most exploited variable, distractor shape, is used as the explicit bias. In the second experiment, the two most exploited variables, distractor shape and texture,

Table 2: Mean of head and tail accuracies on GQA, considering different variables as explicit biases.

Methods	Head/Tail (2 groups)	Answer Class (1833 groups)	Global Group (115 groups)	Local Group (133328 groups)
StdM		44.8		
Up Wt [56]	43.3	26.0	26.4	24.2
GDRO [55]	46.9	28.6	10.8	19.4
RUBi [13]	44.1	N/A	5.6	22.6
LNL [38]	42.9	N/A	32.4	10.7
IRMv1 [5]	47.2	35.8	40.4	33.8
LFF [46]		45.1		
SD [50]		46.9		

are used as explicit biases. This is repeated until all seven variables are used². Note that conducting the seventh experiment entails annotating each instance with every possible source of bias. While this may not be realistic in practice, such a controlled setup will reveal if the explicit methods can generalize when they have complete information about every source of bias. For ease of analysis, we define majority/minority groups with respect to each bias variable, e.g., if most 0s are blue and most 1s are green, then the majority group with respect to digit color comprises of blue 0s, green 1s, etc., while the minority group contains the remaining instances.

To test scalability on a natural dataset, we conduct four experiments per explicit method on GQA-OOD with the explicit bias variables: a) head/tail (2 groups), b) answer class (1833 groups), c) global group (115 groups), and d) local group (133328 groups). Unlike Biased MNIST, we do not test with combinations of these variables since the last three variables already entail generalization to many groups.

Results. We find that implicit methods either improve or are comparable with StdM, but most explicit methods fail when asked to generalize to multiple bias variables and a large number of groups, even when the bias variables are explicitly provided. As shown in Fig. 5, all explicit methods are below StdM on Biased MNIST. Barring LNL and Up Wt, which improve over StdM when $|b_{expl.}| = 1$ and $|b_{expl.}| \geq 6$ respectively, the other explicit methods obtain decreased accuracy as the number of explicit bias variables increases. Because the implicit methods do not rely on the choice of explicit biases, we simply repeat the same accuracy across x-axis. Among the implicit methods, LFF obtains the highest improvement, whereas SD is close to StdM.

Results for GQA-OOD are similar, with explicit methods failing to scale up to a large number of groups, while implicit methods show some improvements over StdM. As shown

²The exact order is given in the Appendix.

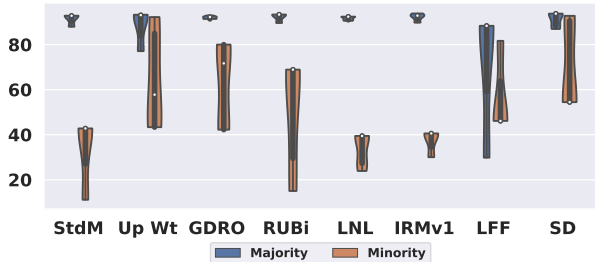


Figure 6: Range of minority (blond haired males) and majority (mean over rest of the groups) test accuracies on CelebA when varying the validation distribution from $\alpha = -1$ (inverted train bias) to $\alpha = 2$ (increased train bias).

in Table 2, when the number of groups is small, i.e., when using a head/tail binary indicator as the explicit bias, explicit methods remain comparable or even outperform StdM, but when the number of groups grow to hundreds and thousands, they fail. IRMv1 and GDRO obtain the highest improvements of 2.4% and 2.1% over StdM, respectively, with the binary head/tail bias, but they show large drops when using answer class, global group or local group as explicit bias variables. Some drops are extreme, e.g., RUBi drops 39% when using global group as the explicit bias variable.

6.4. Robustness to Model Selection Criteria

Question 4: Can the methods generalize to the test set without being tuned on the test distribution? Do they exhibit robustness across wide range of hyperparameters?

Assuming access to the test distribution is unrealistic and can result in models being right for the wrong reasons [64]. Rather, it is ideal if methods can generalize without being tuned on the test distribution. We study this capability by comparing robustness to varying tuning distributions. We compute $Acc_{val}(\alpha)$, with $\alpha \in \{-1.0, -0.5, 0.0, 0.5, 1.0, 1.5, 2.0\}$ using the same validation set, and choose from models trained with different hyperparameters: $learning\ rate \in \{10^{-3}, 10^{-4}, 10^{-5}\}$ and $weight\ decay \in \{10^{-1}, 10^{-3}, 10^{-5}\}$. Here, $\alpha = -1$ inverts the train priors and $\alpha = 2$ amplifies them, but ideally, the methods should behave robustly across the entire range of α 's. We perform this study for CelebA and Biased MNIST.

Results. For CelebA, methods generally show large variance on the minority patterns (blond haired male celebrities), and lower variance on the majority patterns (mean over rest of the groups), whereas for Biased MNIST, we find that methods only work for certain set of hyperparameters and show degraded results on both majority/minority patterns if the hyperparameters change. As illustrated by the violin plots of CelebA's unbiased test accuracies in Fig. 6, LNL and IRMv1 have the lowest variance, but neither improves over StdM. Up Wt, GDRO and RUBi show the largest variances

for the minority group, indicating they are highly sensitive to the choice of tuning distribution. For LFF, we found high variance for both majority and minority patterns. In fact, we were unable to replicate the published LFF results, with $\gamma = 0.7$ yielding a high accuracy (86%) on the rarest group, but low accuracies on the rest. After tuning it, we found that $\gamma = 0.1$ gave the best unbiased test accuracy.

Interestingly, for Biased MNIST we found that $learning\ rate = 10^{-3}$ and $weight\ decay = 10^{-5}$ worked best for all methods. Even though Up Wt and GDRO are known to generalize to minority groups when using a low learning rate and high weight decay [56], we did not observe this for Biased MNIST. We hypothesize that when multiple sources of bias are present, as in Biased MNIST, methods have multiple ways of predicting the classes, some of which maybe easier to learn than the others. When the hyperparameters are suitable to exploit these biases, methods obtain their best accuracies, which are still lower than StdM.

7. Discussion

Our study demonstrates that systems are highly sensitive to the tuning distribution, that explicit methods cannot handle multiple bias sources, and that more rigorous analysis is critical for bias mitigation algorithms for future progress. Based on our results, we argue that the community should focus on implicit methods, rather than explicit, not only because explicit methods require additional annotations, but also because they perform worse on realistic settings.

We make the following recommendations:

1. Compare against multiple state-of-the-art methods under fair settings.
2. Test on datasets that enable control over the number and degrees of biases, including realistic datasets.
3. Analyze generalization to both explicit and implicit sources of bias.
4. Be forthcoming about whether test distribution was used for model selection and compare robustness to tuning distributions that differ from the test.

If these guidelines are adopted, we believe significant progress can be made so that bias mitigation algorithms can have real-world benefit for deployed systems.

We have pointed to issues with existing bias mitigation approaches, which alter the loss or use resampling. An orthogonal avenue for attacking bias mitigation is to use alternative architectures. Neuro-symbolic and graph-based systems could be created that focus on learning and grounding predictions on structured concepts, which have shown promising generalization capabilities [68, 44, 35, 25, 60]. Causality is another relevant line of research, where the goal is to uncover the underlying causal mechanisms [49, 45, 9, 2].

Discovery and usage of causal concepts is a promising direction for building robust systems. These areas have not been explicitly studied for their ability to overcome dataset bias.

Acknowledgements. This work was supported in part by the DARPA/SRI Lifelong Learning Machines program [HR0011-18-C-0051], AFOSR grant [FA9550-18-1-0121], and NSF award #1909696. The views and conclusions contained herein are those of the authors and should not be interpreted as representing the official policies or endorsements of any sponsor.

References

- [1] E. Adeli, Qingyu Zhao, A. Pfefferbaum, E. Sullivan, Li Fei-Fei, Juan Carlos Niebles, and K. Pohl. Bias-resilient neural network. *ArXiv*, abs/1910.03676, 2019. [3](#)
- [2] Vedika Agarwal, Rakshith Shetty, and Mario Fritz. Towards causal VQA: revealing and reducing spurious correlations by invariant and covariant semantic editing. In *2020 IEEE/CVF Conference on Computer Vision and Pattern Recognition, CVPR 2020, Seattle, WA, USA, June 13-19, 2020*, pages 9687–9695. IEEE, 2020. [8](#)
- [3] Aishwarya Agrawal, Dhruv Batra, Devi Parikh, and Anirudha Kembhavi. Don’t just assume; look and answer: Overcoming priors for visual question answering. In *2018 IEEE Conference on Computer Vision and Pattern Recognition, CVPR 2018, Salt Lake City, UT, USA, June 18-22, 2018*, pages 4971–4980. IEEE Computer Society, 2018. [3](#)
- [4] Peter Anderson, Xiaodong He, Chris Buehler, Damien Teney, Mark Johnson, Stephen Gould, and Lei Zhang. Bottom-up and top-down attention for image captioning and visual question answering. In *2018 IEEE Conference on Computer Vision and Pattern Recognition, CVPR 2018, Salt Lake City, UT, USA, June 18-22, 2018*, pages 6077–6086. IEEE Computer Society, 2018. [5](#)
- [5] Martin Arjovsky, Léon Bottou, Ishaan Gulrajani, and David Lopez-Paz. Invariant risk minimization. *arXiv preprint arXiv:1907.02893*, 2019. [2](#), [4](#), [6](#), [7](#), [A18](#)
- [6] Hyojin Bahng, Sanghyuk Chun, Sangdoon Yun, Jaegul Choo, and Seong Joon Oh. Learning de-biased representations with biased representations. In *Proceedings of the 37th International Conference on Machine Learning, ICML 2020, 13-18 July 2020, Virtual Event*, volume 119 of *Proceedings of Machine Learning Research*, pages 528–539. PMLR, 2020. [2](#)
- [7] Hyojin Bahng, Sanghyuk Chun, Sangdoon Yun, Jaegul Choo, and Seong Joon Oh. Learning de-biased representations with biased representations. In *Proceedings of the 37th International Conference on Machine Learning, ICML 2020, 13-18 July 2020, Virtual Event*, volume 119 of *Proceedings of Machine Learning Research*, pages 528–539. PMLR, 2020. [4](#)
- [8] Solon Barocas and Andrew D Selbst. Big data’s disparate impact. *Calif. L. Rev.*, 104:671, 2016. [1](#)
- [9] Alexis Bellot and Mihaela van der Schaar. Accounting for unobserved confounding in domain generalization. *arXiv preprint arXiv:2007.10653*, 2020. [8](#)
- [10] Shai Ben-David, John Blitzer, Koby Crammer, Fernando Pereira, et al. Analysis of representations for domain adaptation. *Advances in neural information processing systems*, 19:137, 2007. [2](#)
- [11] Aharon Ben-Tal, Dick Den Hertog, Anja De Waegenare, Bertrand Melenberg, and Gijs Rennen. Robust solutions of optimization problems affected by uncertain probabilities. *Management Science*, 59(2):341–357, 2013. [3](#)
- [12] Tolga Bolukbasi, Kai-Wei Chang, James Y. Zou, Venkatesh Saligrama, and Adam Tauman Kalai. Man is to computer programmer as woman is to homemaker? debiasing word embeddings. In Daniel D. Lee, Masashi Sugiyama, Ulrike von Luxburg, Isabelle Guyon, and Roman Garnett, editors, *Advances in Neural Information Processing Systems 29: Annual Conference on Neural Information Processing Systems 2016, December 5-10, 2016, Barcelona, Spain*, pages 4349–4357, 2016. [3](#)
- [13] Rémi Cadène, Corentin Dancette, Hedi Ben-younes, Matthieu Cord, and Devi Parikh. RUBi: Reducing Unimodal Biases for Visual Question Answering. In Hanna M. Wallach, Hugo Larochelle, Alina Beygelzimer, Florence d’Alché-Buc, Emily B. Fox, and Roman Garnett, editors, *Advances in Neural Information Processing Systems 32: Annual Conference on Neural Information Processing Systems 2019, NeurIPS 2019, December 8-14, 2019, Vancouver, BC, Canada*, pages 839–850, 2019. [3](#), [6](#), [7](#), [A18](#)
- [14] Robert Challen, Joshua Denny, Martin Pitt, Luke Gompels, Tom Edwards, and Krasimira Tsaneva-Atanasova. Artificial intelligence, bias and clinical safety. *BMJ Quality & Safety*, 28(3):231–237, 2019. [1](#)
- [15] Nitesh V Chawla, Kevin W Bowyer, Lawrence O Hall, and W Philip Kegelmeyer. Smote: synthetic minority over-sampling technique. *Journal of artificial intelligence research*, 16:321–357, 2002. [3](#)
- [16] Yo Joong Choe, Jiyeon Ham, and Kyubyong Park. An empirical study of invariant risk minimization. *ICML 2020 Workshop on Uncertainty and Robustness in Deep Learning*, 2020. [4](#)
- [17] Alexandra Chouldechova. Fair prediction with disparate impact: A study of bias in recidivism prediction instruments. *Big data*, 5(2):153–163, 2017. [1](#)
- [18] Christopher Clark, Mark Yatskar, and Luke Zettlemoyer. Don’t take the easy way out: Ensemble based methods for avoiding known dataset biases. In *Proceedings of the 2019 Conference on Empirical Methods in Natural Language Processing and the 9th International Joint Conference on Natural Language Processing (EMNLP-IJCNLP)*, pages 4069–4082, Hong Kong, China, 2019. Association for Computational Linguistics. [3](#)
- [19] Christopher Clark, Mark Yatskar, and Luke Zettlemoyer. Learning to model and ignore dataset bias with mixed capacity ensembles. In *Findings of the Association for Computational Linguistics: EMNLP 2020*, pages 3031–3045, Online, 2020. Association for Computational Linguistics. [2](#), [4](#)
- [20] Remi Tachet des Combes, Mohammad Pezeshki, Samira Shabaniyan, Aaron Courville, and Yoshua Bengio. On the learning dynamics of deep neural networks. *arXiv preprint arXiv:1809.06848*, 2018. [4](#)

- [21] Yin Cui, Menglin Jia, Tsung-Yi Lin, Yang Song, and Serge J. Belongie. Class-balanced loss based on effective number of samples. In *IEEE Conference on Computer Vision and Pattern Recognition, CVPR 2019, Long Beach, CA, USA, June 16-20, 2019*, pages 9268–9277. Computer Vision Foundation / IEEE, 2019. [3](#)
- [22] Anupam Datta, Matthew Fredrikson, Gihyuk Ko, Piotr Mardziel, and Shayak Sen. Use privacy in data-driven systems: Theory and experiments with machine learnt programs. In *Proceedings of the 2017 ACM SIGSAC Conference on Computer and Communications Security*, pages 1193–1210, 2017. [1](#)
- [23] Erick Delage and Yinyu Ye. Distributionally robust optimization under moment uncertainty with application to data-driven problems. *Operations research*, 58(3):595–612, 2010. [3](#)
- [24] John C Duchi, Peter W Glynn, and Hongseok Namkoong. Statistics of robust optimization: A generalized empirical likelihood approach. *Mathematics of Operations Research*, 2021. [3](#)
- [25] Difei Gao, Ke Li, Ruiping Wang, Shiguang Shan, and Xilin Chen. Multi-modal graph neural network for joint reasoning on vision and scene text. In *2020 IEEE/CVF Conference on Computer Vision and Pattern Recognition, CVPR 2020, Seattle, WA, USA, June 13-19, 2020*, pages 12743–12753. IEEE, 2020. [8](#)
- [26] Gabriel Grand and Yonatan Belinkov. Adversarial regularization for visual question answering: Strengths, shortcomings, and side effects. In *Proceedings of the Second Workshop on Shortcomings in Vision and Language*, pages 1–13, Minneapolis, Minnesota, 2019. Association for Computational Linguistics. [3](#), [4](#)
- [27] Haibo He, Yang Bai, Eduardo A Garcia, and Shutao Li. Adasyn: Adaptive synthetic sampling approach for imbalanced learning. In *2008 IEEE international joint conference on neural networks (IEEE world congress on computational intelligence)*, pages 1322–1328. IEEE, 2008. [3](#)
- [28] Haibo He and Eduardo A Garcia. Learning from imbalanced data. *IEEE Transactions on knowledge and data engineering*, 21(9):1263–1284, 2009. [3](#)
- [29] He He, Sheng Zha, and Haohan Wang. Unlearn dataset bias in natural language inference by fitting the residual. In *Proceedings of the 2nd Workshop on Deep Learning Approaches for Low-Resource NLP (DeepLo 2019)*, pages 132–142, Hong Kong, China, 2019. Association for Computational Linguistics. [3](#)
- [30] Kaiming He, Xiangyu Zhang, Shaoqing Ren, and Jian Sun. Deep residual learning for image recognition. In *2016 IEEE Conference on Computer Vision and Pattern Recognition, CVPR 2016, Las Vegas, NV, USA, June 27-30, 2016*, pages 770–778. IEEE Computer Society, 2016. [5](#)
- [31] Katherine L Hermann and Andrew K Lampinen. What shapes feature representations? exploring datasets, architectures, and training. *NeurIPS*, 2020. [4](#)
- [32] Geoffrey E Hinton. Training products of experts by minimizing contrastive divergence. *Neural computation*, 14(8):1771–1800, 2002. [3](#)
- [33] Weihua Hu, Gang Niu, Issei Sato, and Masashi Sugiyama. Does distributionally robust supervised learning give robust classifiers? In Jennifer G. Dy and Andreas Krause, editors, *Proceedings of the 35th International Conference on Machine Learning, ICML 2018, Stockholmsmässan, Stockholm, Sweden, July 10-15, 2018*, volume 80 of *Proceedings of Machine Learning Research*, pages 2034–2042. PMLR, 2018. [3](#)
- [34] Drew A. Hudson and Christopher D. Manning. GQA: A new dataset for real-world visual reasoning and compositional question answering. In *IEEE Conference on Computer Vision and Pattern Recognition, CVPR 2019, Long Beach, CA, USA, June 16-20, 2019*, pages 6700–6709. Computer Vision Foundation / IEEE, 2019. [5](#)
- [35] Drew A. Hudson and Christopher D. Manning. Learning by abstraction: The neural state machine. In Hanna M. Wallach, Hugo Larochelle, Alina Beygelzimer, Florence d’Alché-Buc, Emily B. Fox, and Roman Garnett, editors, *Advances in Neural Information Processing Systems 32: Annual Conference on Neural Information Processing Systems 2019, NeurIPS 2019, December 8-14, 2019, Vancouver, BC, Canada*, pages 5901–5914, 2019. [8](#)
- [36] Kushal Kafle, Robik Shrestha, and Christopher Kanan. Challenges and prospects in vision and language research. *Frontiers in Artificial Intelligence*, 2:28, 2019. [1](#)
- [37] Corentin Kervadec, Grigory Antipov, Moez Baccouche, and Christian Wolf. Roses are red, violets are blue... but should vqa expect them to? *arXiv preprint arXiv:2006.05121*, 2020. [5](#), [A13](#)
- [38] Byungju Kim, Hyunwoo Kim, Kyungsu Kim, Sungjin Kim, and Junmo Kim. Learning not to learn: Training deep neural networks with biased data. In *IEEE Conference on Computer Vision and Pattern Recognition, CVPR 2019, Long Beach, CA, USA, June 16-20, 2019*, pages 9012–9020. Computer Vision Foundation / IEEE, 2019. [1](#), [2](#), [4](#), [6](#), [7](#), [A18](#)
- [39] David Krueger, Ethan Caballero, Joern-Henrik Jacobsen, Amy Zhang, Jonathan Binas, Dinghuai Zhang, Remi Le Priol, and Aaron Courville. Out-of-distribution generalization via risk extrapolation (rex). *arXiv preprint arXiv:2003.00688*, 2020. [4](#)
- [40] Yingwei Li, Yi Li, and Nuno Vasconcelos. Resound: Towards action recognition without representation bias. In *Proceedings of the European Conference on Computer Vision (ECCV)*, pages 513–528, 2018. [3](#)
- [41] Yi Li and Nuno Vasconcelos. REPAIR: removing representation bias by dataset resampling. In *IEEE Conference on Computer Vision and Pattern Recognition, CVPR 2019, Long Beach, CA, USA, June 16-20, 2019*, pages 9572–9581. Computer Vision Foundation / IEEE, 2019. [2](#), [3](#)
- [42] Tsung-Yi Lin, Priya Goyal, Ross B. Girshick, Kaiming He, and Piotr Dollár. Focal loss for dense object detection. In *IEEE International Conference on Computer Vision, ICCV 2017, Venice, Italy, October 22-29, 2017*, pages 2999–3007. IEEE Computer Society, 2017. [3](#)
- [43] Ziwei Liu, Ping Luo, Xiaogang Wang, and Xiaoou Tang. Large-scale celebfaces attributes (celeba) dataset. *Retrieved August, 15:2018*, 2018. [1](#), [5](#)
- [44] Jiayuan Mao, Chuang Gan, Pushmeet Kohli, Joshua B. Tenenbaum, and Jiajun Wu. The neuro-symbolic concept learner: Interpreting scenes, words, and sentences from natural su-

- pervision. In *7th International Conference on Learning Representations, ICLR 2019, New Orleans, LA, USA, May 6-9, 2019*. OpenReview.net, 2019. [8](#)
- [45] Nicolai Meinshausen. Causality from a distributional robustness point of view. In *2018 IEEE Data Science Workshop (DSW)*, pages 6–10. IEEE, 2018. [8](#)
- [46] Junhyun Nam, Hyuntak Cha, Sungsoo Ahn, Jaeho Lee, and Jinwoo Shin. Learning from failure: Training debiased classifier from biased classifier. In *Advances in Neural Information Processing Systems*, 2020. [1](#), [2](#), [4](#), [5](#), [6](#), [7](#), [A18](#)
- [47] Hongseok Namkoong and John C. Duchi. Stochastic gradient methods for distributionally robust optimization with f-divergences. In Daniel D. Lee, Masashi Sugiyama, Ulrike von Luxburg, Isabelle Guyon, and Roman Garnett, editors, *Advances in Neural Information Processing Systems 29: Annual Conference on Neural Information Processing Systems 2016, December 5-10, 2016, Barcelona, Spain*, pages 2208–2216, 2016. [3](#)
- [48] Peter A Noseworthy, Zachi I Attia, LaPrincess C Brewer, Sharonne N Hayes, Xiaoxi Yao, Suraj Kapa, Paul A Friedman, and Francisco Lopez-Jimenez. Assessing and mitigating bias in medical artificial intelligence: the effects of race and ethnicity on a deep learning model for ecg analysis. *Circulation: Arrhythmia and Electrophysiology*, 13(3):e007988, 2020. [1](#)
- [49] Jonas Peters, Peter Bühlmann, and Nicolai Meinshausen. Causal inference by using invariant prediction: identification and confidence intervals. *Journal of the Royal Statistical Society. Series B (Statistical Methodology)*, pages 947–1012, 2016. [8](#)
- [50] Mohammad Pezeshki, Sékou-Oumar Kaba, Yoshua Bengio, Aaron Courville, Doina Precup, and Guillaume Lajoie. Gradient starvation: A learning proclivity in neural networks. *arXiv preprint arXiv:2011.09468*, 2020. [1](#), [2](#), [4](#), [5](#), [6](#), [7](#), [A18](#)
- [51] Oskar Pfungst. *Clever Hans:(the horse of Mr. Von Osten.) a contribution to experimental animal and human psychology*. Holt, Rinehart and Winston, 1911. [2](#)
- [52] Sainandan Ramakrishnan, Aishwarya Agrawal, and Stefan Lee. Overcoming language priors in visual question answering with adversarial regularization. In Samy Bengio, Hanna M. Wallach, Hugo Larochelle, Kristen Grauman, Nicolò Cesa-Bianchi, and Roman Garnett, editors, *Advances in Neural Information Processing Systems 31: Annual Conference on Neural Information Processing Systems 2018, NeurIPS 2018, December 3-8, 2018, Montréal, Canada*, pages 1548–1558, 2018. [3](#), [4](#)
- [53] Elan Rosenfeld, Pradeep Ravikumar, and Andrej Risteski. The risks of invariant risk minimization. *arXiv preprint arXiv:2010.05761*, 2020. [4](#)
- [54] Swati Sachan, Jian-Bo Yang, Dong-Ling Xu, David Erasó Benavides, and Yang Li. An explainable ai decision-support-system to automate loan underwriting. *Expert Systems with Applications*, 144:113100, 2020. [1](#)
- [55] Shiori Sagawa, Pang Wei Koh, Tatsunori B Hashimoto, and Percy Liang. Distributionally robust neural networks for group shifts: On the importance of regularization for worst-case generalization. *arXiv preprint arXiv:1911.08731*, 2019. [1](#), [3](#), [5](#), [6](#), [7](#), [A18](#)
- [56] Shiori Sagawa, Aditi Raghunathan, Pang Wei Koh, and Percy Liang. An investigation of why overparameterization exacerbates spurious correlations. In *Proceedings of the 37th International Conference on Machine Learning, ICML 2020, 13-18 July 2020, Virtual Event*, volume 119 of *Proceedings of Machine Learning Research*, pages 8346–8356. PMLR, 2020. [5](#), [6](#), [7](#), [8](#), [A18](#)
- [57] Victor Sanh, Thomas Wolf, Yonatan Belinkov, and Alexander M Rush. Learning from others’ mistakes: Avoiding dataset biases without modeling them. *arXiv preprint arXiv:2012.01300*, 2020. [4](#)
- [58] Ramprasaath Ramasamy Selvaraju, Stefan Lee, Yilin Shen, Hongxia Jin, Shalini Ghosh, Larry P. Heck, Dhruv Batra, and Devi Parikh. Taking a HINT: leveraging explanations to make vision and language models more grounded. In *2019 IEEE/CVF International Conference on Computer Vision, ICCV 2019, Seoul, Korea (South), October 27 - November 2, 2019*, pages 2591–2600. IEEE, 2019. [5](#)
- [59] Harshay Shah, Kaustav Tamuly, Aditi Raghunathan, Prateek Jain, and Praneeth Netrapalli. The pitfalls of simplicity bias in neural networks. *arXiv preprint arXiv:2006.07710*, 2020. [2](#), [4](#)
- [60] Jiaxin Shi, Hanwang Zhang, and Juanzi Li. Explainable and explicit visual reasoning over scene graphs. In *IEEE Conference on Computer Vision and Pattern Recognition, CVPR 2019, Long Beach, CA, USA, June 16-20, 2019*, pages 8376–8384. Computer Vision Foundation / IEEE, 2019. [8](#)
- [61] Robik Shrestha, Kushal Kafle, and Christopher Kanan. Answer them all! toward universal visual question answering models. In *IEEE Conference on Computer Vision and Pattern Recognition, CVPR 2019, Long Beach, CA, USA, June 16-20, 2019*, pages 10472–10481. Computer Vision Foundation / IEEE, 2019. [3](#)
- [62] Robik Shrestha, Kushal Kafle, and Christopher Kanan. A negative case analysis of visual grounding methods for VQA. In *Proceedings of the 58th Annual Meeting of the Association for Computational Linguistics*, pages 8172–8181, Online, July 2020. Association for Computational Linguistics. [2](#)
- [63] Damien Teney, Ehsan Abbasnejad, and Anton van den Hengel. Unshuffling data for improved generalization. *arXiv preprint arXiv:2002.11894*, 2020. [4](#)
- [64] Damien Teney, Kushal Kafle, Robik Shrestha, Ehsan Abbasnejad, Christopher Kanan, and Anton van den Hengel. On the value of out-of-distribution testing: An example of goodhart’s law. 2020. [2](#), [8](#)
- [65] Prasetya Ajie Utama, Nafise Sadat Moosavi, and Iryna Gurevych. Towards debiasing NLU models from unknown biases. In *Proceedings of the 2020 Conference on Empirical Methods in Natural Language Processing (EMNLP)*, pages 7597–7610, Online, 2020. Association for Computational Linguistics. [2](#), [4](#)
- [66] Jialin Wu, Liyan Chen, and Raymond J Mooney. Improving vqa and its explanations by comparing competing explanations. *arXiv preprint arXiv:2006.15631*, 2020. [5](#)
- [67] Chuanlong Xie, Fei Chen, Yue Liu, and Zhenguo Li. Risk variance penalization: From distributional robustness to causality. *arXiv preprint arXiv:2006.07544*, 2020. [4](#)

- [68] Kexin Yi, Jiajun Wu, Chuang Gan, Antonio Torralba, Pushmeet Kohli, and Josh Tenenbaum. Neural-symbolic VQA: disentangling reasoning from vision and language understanding. In Samy Bengio, Hanna M. Wallach, Hugo Larochelle, Kristen Grauman, Nicolò Cesa-Bianchi, and Roman Garnett, editors, *Advances in Neural Information Processing Systems 31: Annual Conference on Neural Information Processing Systems 2018, NeurIPS 2018, December 3-8, 2018, Montréal, Canada*, pages 1039–1050, 2018. [8](#)
- [69] Brian Hu Zhang, Blake Lemoine, and Margaret Mitchell. Mitigating unwanted biases with adversarial learning. In *Proceedings of the 2018 AAAI/ACM Conference on AI, Ethics, and Society*, pages 335–340, 2018. [1](#), [3](#), [4](#)
- [70] Zhilu Zhang and Mert R. Sabuncu. Generalized cross entropy loss for training deep neural networks with noisy labels. In Samy Bengio, Hanna M. Wallach, Hugo Larochelle, Kristen Grauman, Nicolò Cesa-Bianchi, and Roman Garnett, editors, *Advances in Neural Information Processing Systems 31: Annual Conference on Neural Information Processing Systems 2018, NeurIPS 2018, December 3-8, 2018, Montréal, Canada*, pages 8792–8802, 2018. [4](#)
- [71] Jieyu Zhao, Tianlu Wang, Mark Yatskar, Vicente Ordonez, and Kai-Wei Chang. Men also like shopping: Reducing gender bias amplification using corpus-level constraints. In *Proceedings of the 2017 Conference on Empirical Methods in Natural Language Processing*, pages 2979–2989, Copenhagen, Denmark, 2017. Association for Computational Linguistics. [1](#)
- [72] Yang Zou, Zhiding Yu, BVK Vijaya Kumar, and Jinsong Wang. Unsupervised domain adaptation for semantic segmentation via class-balanced self-training. In *Proceedings of the European conference on computer vision (ECCV)*, pages 289–305, 2018. [3](#)

A. Appendix

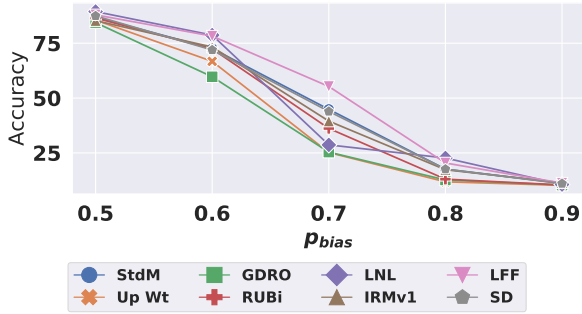


Figure A7: Unbiased accuracy on Biased MNIST as a function p_{bias} .

A.1. Additional Results

We now provide additional results for all datasets, that provide further details for the results presented in Sec. 6.

Biased MNIST. First, we show the unbiased accuracy as a function of p_{bias} in Fig. A7. None of the methods exhibit robustness across the range of p_{bias} values, with all methods showing drops in the unbiased accuracy as p_{bias} increases from 0.5 to 0.9. Second, in Fig. A8, we show the unbiased accuracies as functions of learning rate and weight decay, when p_{bias} is set to 0.7. The figure on the left shows unbiased accuracies as a function of learning rate with a fixed weight decay of 10^{-5} and the figure on the right shows unbiased accuracies as a function of weight decay, with learning rate set to 10^{-3} . Barring Up Wt, all methods show highest unbiased accuracies at learning rate = 10^{-3} and weight decay = 10^{-5} , and show large drops with other values, indicating high sensitivities to hyperparameters.

Third, in Table. A4, we compare the explicit methods with each other, when considering each of the seven variables as explicit bias variables ($b_{expl.}$) in separate experiments. For the explicit methods, variables apart from $b_{expl.}$ act as implicit biases, whereas implicit methods are not affected by the choice of the explicit variables. As previously discussed in Sec. 6.2, Up Wt, GDRO and RUBi show higher majority/minority difference for $b_{expl.}$ as compared to other variables, and all explicit methods are below StdM in terms of unbiased accuracies. Finally, in Table. A5, we show the per variable majority/minority accuracies when considering combinations of variables as explicit biases. As discussed in Sec. 6.3, explicit methods barring Up Wt fail when multiple variables are specified as explicit bias variables. The results have been averaged across three runs for both tables. We provide a ten samples for each digit in Fig. A10.

CelebA. We show accuracy for each group of CelebA in Table. A3. SD and GDRO obtain the highest accuracies. As discussed previously, we observe trade-offs between blond

Table A3: Per group accuracies on CelebA.

Groups/ Methods	Male		Non-Male		Unbiased Accuracy
	Non- Blond	Blond	Non- Blond	Blond	
StdM	<u>99.3</u>	42.8	<u>95.9</u>	83.3	80.3
Up Wt	89.3	77.8	87.4	95.0	87.4
GDRO	91.2	<u>80.0</u>	90.9	<u>92.1</u>	88.5
RUBi	<u>96.6</u>	68.9	<u>94.3</u>	89.1	87.2
LNL	99.1	39.4	95.4	82.8	79.2
IRMv1	99.1	40.6	<u>95.9</u>	83.6	79.8
LFF	96.0	46.1	90.4	80.0	77.8
SD	96.4	<u>73.3</u>	88.0	<u>96.6</u>	<u>88.6</u>

and non-blond classes with the improvements in the rare blond class incurring degradations in the non-blond class.

GQA-OOD. GQA-OOD [37] defines the tail accuracy (Acc-tail) metric which is computed on the samples of the tail of the answer class distribution. Specifically, an answer class a_i is considered to be a tail class for a local group if:

$$|a_i| \leq (1 + \beta)\mu(a),$$

where, $|a_i|$ is the number of instances for answer a_i in the given group, $\mu(a)$ is the mean number of answers in the group and β can be used to control the tail size. In Fig. A9, we plot the tail accuracies at different tail sizes, considering different explicit bias variables for the explicit methods. For implicit methods: StdM, LFF and SD, same tail accuracies are repeated on all four charts since they are not affected by the choice of explicit variables during training. Explicit methods fail when the explicit variables entail generalization to large number of groups, whereas implicit methods are close to or above StdM.

A.2. Hyperparameters and Other Details

We select hyperparameters based on the best unbiased validation set accuracy on each dataset, which is reflective of the unbiased test distribution. For all datasets and methods, we first perform a grid search over the learning rates $\in \{1e-3, 1e-4, 1e-5\}$ and weight decays $\in \{0, 0.1, 1e-3, 1e-5\}$, and then tune the method-specific hyperparameters. For Biased MNIST, the hyperparameters were selected using single run, considering ‘distractor shape’ as the explicit bias variable for explicit methods. For CelebA, they were selected based on the unbiased accuracy/mean per group on the validation set and for GQA-OOD, they were selected based on the best mean head/tail accuracy when setting $\beta = 0.2$ (the default value in the original paper).

Next we specify the ranges considered for method-specific hyperparameters. For GDRO, we search the group weight step size between $\{0.001, 0.01, 0.1\}$. For LNL, we perform a grid search over gradient reversal weights

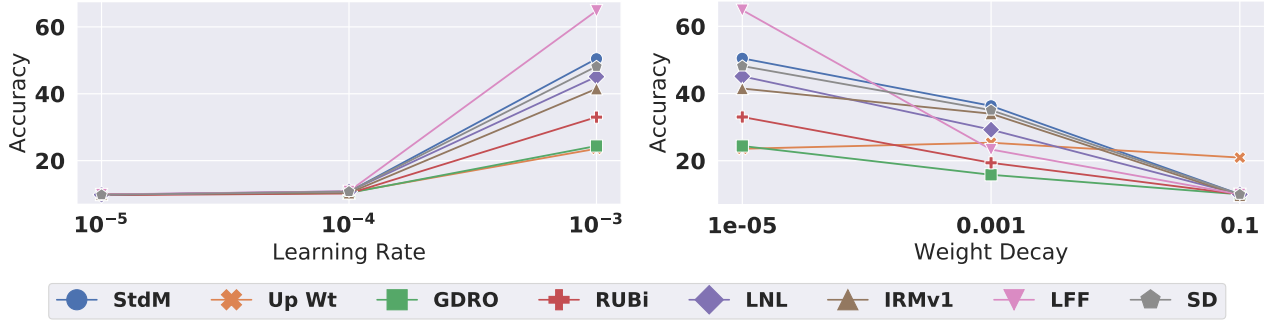


Figure A8: Unbiased test accuracy (mean per group) as a function of learning rate and weight decay (using single random seed).

$\lambda_{adv} \in \{-1.0, -0.1, -0.01\}$ and entropy loss weights $\lambda_{ent} \in \{1.0, 0.1, 0.01, 0\}$. For IRMv1, we search for λ_{grad} values from $\{1, 10, 100, 1000, 10000\}$. The original implementation of IRMv1 samples from all environments in a single mini-batch during training. While this is feasible for small scale problems with few environments e.g., four environments/explicit groups for CelebA, it is computationally infeasible for Biased MNIST and GQA, where the number of environments is larger than the batch size itself. So, for Biased MNIST and GQA, we sample from 16 randomly selected groups or environments within each mini-batch during training. This implies that our implementation of IRMv1 samples uniformly from all environments.

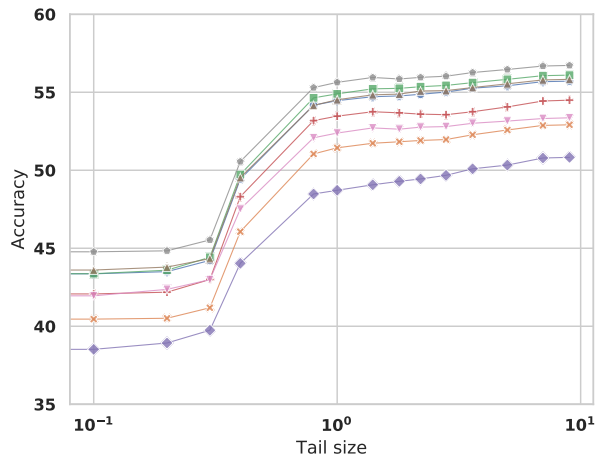
Even though the original paper proposing LFF uses a fixed $\gamma = 0.7$ for all datasets, we search over $\gamma \in \{0.1, 0.3, 0.5, 0.7, 0.9\}$ and find that LFF is indeed sensitive to γ . The default value: $\gamma = 0.7$ is not the optimal value for all cases. For SD, we consider $\gamma, \lambda \in \{10^{-3}, 10^{-2}, 0.1, 1.0, 10.0, 100.0\}$. For CelebA, we use the class-specific γ values specified in the paper and only tune λ . The procedure for obtaining class-specific hyperparameters when there are large number of classes e.g., in GQA however remains unclear for SD. The complete specification of hyperparameters is provided in Table. A6.

Table A4: Majority (Maj.) and Minority (Min.) group accuracies for each variable in Biased MNIST when using one of the seven variables as explicit bias for the explicit methods.

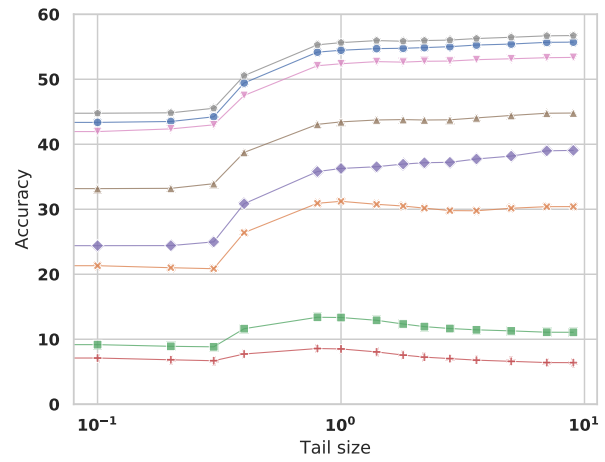
Variables/ Methods	Unbiased Accuracy	Background Color		Digit Color		Digit Position		Distractor Shape		Distractor Color		Texture		Texture Color	
		Maj.	Min.	Maj.	Min.	Maj.	Min.	Maj.	Min.	Maj.	Min.	Maj.	Min.	Maj.	Min.
StdM	42.0	70.3	39.1	74.6	38.7	48.3	41.6	69.2	39.2	68.9	39.4	69.4	39.1	65.2	39.7
$b_{expl.} = \text{Background Color}$															
Up Wt	39.0	42.0	38.9	72.7	35.4	43.3	38.7	71.2	35.6	70.3	35.8	67.6	35.9	65.4	36.2
GDRO	32.8	52.2	30.8	66.8	29.2	37.0	32.5	62.4	29.6	64.1	29.6	64.5	29.3	62.6	29.6
RUBi	47.9	51.9	47.7	78.8	44.6	52.4	47.6	77.4	44.8	77.8	44.9	76.5	44.8	72.9	45.2
LNL	44.0	55.8	43.5	59.7	43.0	46.8	44.5	57.5	43.3	57.6	43.3	56.6	43.3	53.2	43.7
IRMv1	38.0	66.0	35.0	70.5	34.5	41.2	37.8	68.1	34.8	68.3	34.9	64.5	35.1	65.6	35.0
$b_{expl.} = \text{Digit Color}$															
Up Wt	19.4	48.6	16.1	22.8	19.0	21.5	19.2	52.0	15.7	47.7	16.3	50.5	15.7	44.9	16.5
GDRO	22.6	50.1	19.6	45.7	20.1	25.7	22.3	52.1	19.3	52.3	19.4	52.0	19.2	51.5	19.4
RUBi	24.0	54.5	20.6	27.9	23.6	25.0	23.9	57.3	20.2	55.4	20.6	55.4	20.3	52.6	20.7
LNL	40.2	53.7	39.5	57.9	39.0	46.2	40.3	56.1	39.2	55.1	39.4	56.1	39.2	50.9	39.8
IRMv1	40.9	66.8	38.4	72.3	37.8	43.8	41.0	71.1	37.9	68.9	38.3	67.8	38.2	66.5	38.4
$b_{expl.} = \text{Digit Position}$															
Up Wt	21.4	46.7	18.6	50.4	18.2	21.9	21.4	53.4	17.8	50.4	18.3	49.0	18.2	45.8	18.6
GDRO	26.8	54.9	23.9	55.4	23.9	27.6	27.0	58.2	23.5	54.9	24.0	54.5	23.9	51.6	24.3
RUBi	26.6	54.9	23.5	59.1	23.0	28.3	26.5	56.8	23.2	56.9	23.4	56.0	23.2	53.5	23.6
LNL	41.4	51.8	40.9	56.6	40.4	46.4	41.5	54.4	40.6	53.7	40.7	52.7	40.7	49.4	41.1
IRMv1	38.1	67.8	35.0	70.8	34.7	42.9	37.8	69.3	34.8	68.0	35.1	67.0	34.9	66.0	35.1
$b_{expl.} = \text{Distractor Shape}$															
Up Wt	21.5	52.0	18.2	56.0	17.8	24.2	21.4	25.6	21.2	53.0	18.2	54.0	17.9	51.9	18.2
GDRO	25.2	54.1	22.2	56.9	21.9	27.9	25.2	48.9	22.8	56.0	22.1	56.0	21.9	52.3	22.4
RUBi	34.5	66.9	31.0	70.9	30.5	35.2	34.5	40.4	33.9	67.7	31.0	67.5	30.7	64.6	31.1
LNL	44.1	55.8	43.1	59.6	42.6	50.5	43.7	57.9	42.8	57.4	42.9	58.8	42.7	55.0	43.1
IRMv1	38.3	67.0	35.5	70.5	35.1	41.5	38.3	69.3	35.2	65.9	35.7	67.9	35.2	64.6	35.7
$b_{expl.} = \text{Distractor Color}$															
Up Wt	40.9	70.1	38.0	70.8	38.0	46.6	40.7	73.0	37.7	44.8	40.9	73.0	37.6	68.5	38.2
GDRO	28.1	58.6	24.8	57.4	24.9	30.4	28.0	62.1	24.4	49.1	25.9	59.1	24.6	55.8	25.1
RUBi	49.5	77.3	46.6	80.1	46.3	54.5	49.1	78.3	46.4	53.8	49.2	77.6	46.4	76.4	46.6
LNL	38.9	52.4	38.2	55.9	37.8	46.0	38.9	56.6	37.7	52.8	38.2	56.0	37.7	51.5	38.3
IRMv1	39.7	66.1	36.8	72.3	36.1	45.1	39.2	68.8	36.5	69.1	36.6	66.4	36.6	64.8	36.9
$b_{expl.} = \text{Texture}$															
Up Wt	29.3	60.8	25.9	66.1	25.4	32.9	29.1	64.6	25.5	62.3	25.9	32.9	29.1	60.7	25.9
GDRO	24.5	54.9	21.3	58.0	21.0	27.3	24.4	56.8	21.1	54.8	21.4	42.7	22.6	51.6	21.6
RUBi	43.1	73.7	39.8	78.5	39.3	44.9	43.1	74.2	39.7	74.8	39.8	48.1	42.7	71.7	40.0
LNL	41.7	55.9	40.8	59.1	40.5	48.4	41.7	56.3	40.8	56.5	40.8	57.1	40.6	53.7	41.0
IRMv1	37.5	64.4	34.6	67.1	34.3	39.5	37.4	68.0	34.2	65.8	34.5	66.2	34.3	62.5	34.8
$b_{expl.} = \text{Texture Color}$															
Up Wt	39.5	71.6	36.1	71.4	36.2	43.7	39.3	70.3	36.3	67.6	36.7	69.4	36.2	42.4	39.4
GDRO	30.4	59.5	27.4	60.7	27.2	33.5	30.3	61.6	27.1	60.9	27.3	61.9	26.9	45.1	28.9
RUBi	46.8	74.0	43.8	76.6	43.5	48.9	46.6	73.8	43.8	74.0	43.9	75.7	43.5	49.2	46.6
LNL	34.3	49.2	33.4	47.9	33.5	41.8	34.2	49.9	33.3	47.8	33.6	48.6	33.4	43.3	34.0
IRMv1	38.5	66.1	35.7	71.0	35.2	43.7	38.3	69.2	35.4	67.6	35.7	68.2	35.4	63.6	36.0
Implicit Methods															
LFF	56.6	71.2	55.4	82.6	54.2	63.8	56.3	77.0	54.8	74.6	55.1	76.2	54.8	75.4	54.9
SD	41.3	69.5	38.3	71.2	38.1	46.3	40.9	72.2	38.0	72.1	38.1	71.1	38.0	70.5	38.2

Table A5: Method accuracies with increasing number of explicit bias variables.

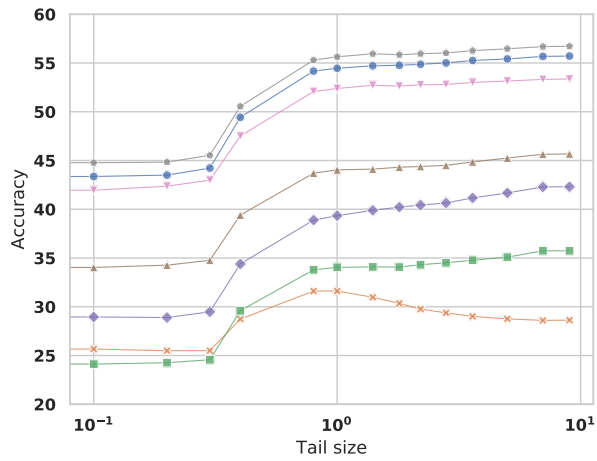
Variables/ Methods	Unbiased Accuracy	Background Color		Digit Color		Digit Position		Distractor Shape		Distractor Color		Texture Pattern		Texture Color	
		Maj.	Min.	Maj.	Min.	Maj.	Min.	Maj.	Min.	Maj.	Min.	Maj.	Min.	Maj.	Min.
StdM	42.0	70.3	39.1	74.6	38.7	48.3	41.6	69.2	39.2	68.9	39.4	69.4	39.1	65.2	39.7
$b_{expl.} = \text{Distractor Shape}$															
Up Wt	21.5	52.0	18.2	56.0	17.8	24.2	21.4	25.6	21.2	53.0	18.2	54.0	17.9	51.9	18.2
GDRO	25.2	54.1	22.2	56.9	21.9	27.9	25.2	48.9	22.8	56.0	22.1	56.0	21.9	52.3	22.4
RUBi	34.5	66.9	31.0	70.9	30.5	35.2	34.5	40.4	33.9	67.7	31.0	67.5	30.7	64.6	31.1
LNL	44.1	55.8	43.1	59.6	42.6	50.5	43.7	57.9	42.8	57.4	42.9	58.8	42.7	55.0	43.1
IRMv1	38.3	67.0	35.5	70.5	35.1	41.5	38.3	69.3	35.2	65.9	35.7	67.9	35.2	64.6	35.7
$b_{expl.} = \text{Distractor Shape+Texture Pattern}$															
Up Wt	16.1	49.0	12.6	51.6	12.3	18.3	16.0	20.6	15.8	50.7	12.5	18.5	16.0	45.3	12.9
GDRO	17.4	43.7	14.6	44.3	14.6	20.1	17.3	42.5	14.8	46.4	14.4	42.6	14.6	41.8	14.8
RUBi	27.9	64.3	24.0	70.9	23.3	32.1	27.6	36.5	27.1	65.9	24.0	34.1	27.4	60.6	24.3
LNL	10.0	14.7	10.5	11.0	10.9	11.3	10.9	12.3	10.8	11.8	10.9	12.9	10.7	11.7	10.9
IRMv1	34.3	64.4	31.2	68.5	30.8	38.5	34.2	63.9	31.3	63.7	31.4	61.3	31.4	62.3	31.4
$b_{expl.} = \text{Distractor Shape+Texture Pattern+Digit Color}$															
Up Wt	12.6	47.7	8.7	20.1	11.8	13.5	12.5	22.9	11.5	45.8	9.0	22.7	11.4	42.3	9.2
GDRO	18.4	44.1	15.6	42.6	15.8	20.0	18.3	44.8	15.5	45.7	15.6	44.2	15.5	43.6	15.7
RUBi	11.0	48.9	6.8	12.9	10.9	11.8	11.0	11.1	11.1	46.8	7.2	11.0	11.1	41.0	7.6
LNL	10.2	15.2	10.6	11.5	11.1	11.7	11.0	11.4	11.1	12.2	11.0	18.4	10.2	15.3	10.6
IRMv1	24.9	57.0	21.4	53.8	21.8	27.6	24.8	52.4	21.9	56.0	21.7	50.7	22.0	55.3	21.6
$b_{expl.} = \text{Distractor Shape+Texture Pattern+Digit Color+Background Color}$															
Up Wt	30.1	54.5	27.6	59.3	27.1	35.0	29.8	56.0	27.4	64.0	26.7	56.3	27.3	63.4	26.5
GDRO	19.9	48.2	17.0	45.3	17.4	22.8	19.9	50.9	16.7	47.4	17.2	46.7	17.1	43.8	17.5
RUBi	10.0	10.3	9.9	11.9	9.7	10.0	10.0	9.2	10.0	59.4	4.6	10.4	9.9	48.0	5.6
LNL	10.0	10.0	11.5	10.6	11.4	11.2	11.4	11.9	11.3	13.0	11.2	11.3	11.4	10.6	11.4
IRMv1	25.6	52.9	22.7	58.1	22.1	30.1	25.2	52.3	22.7	57.5	22.3	52.4	22.6	56.0	22.3
$b_{expl.} = \text{Distractor Shape+Texture Pattern+Digit Color+Background Color+Texture Color}$															
Up Wt	38.8	65.3	36.0	71.4	35.3	42.3	38.5	68.2	35.6	71.0	35.4	67.1	35.6	61.5	36.3
GDRO	21.9	49.9	19.1	47.2	19.4	25.1	21.8	53.2	18.7	50.8	19.1	51.6	18.7	45.6	19.5
RUBi	9.8	10.2	9.7	9.6	9.8	9.8	9.7	8.8	9.8	88.2	1.2	9.7	9.7	9.3	9.8
LNL	10.0	10.0	11.5	10.6	11.4	11.2	11.4	11.9	11.3	13.0	11.2	11.3	11.4	10.6	11.4
IRMv1	28.4	58.7	25.0	61.5	24.7	32.2	28.0	56.6	25.2	59.3	25.1	57.8	25.0	53.5	25.6
$b_{expl.} = \text{Distractor Shape+Texture Pattern+Digit Color+Background Color+Texture Color+Distractor Color}$															
Up Wt	43.2	71.0	40.4	75.3	39.9	47.3	43.1	72.1	40.2	69.7	40.6	72.8	40.0	68.5	40.6
GDRO	19.7	47.3	16.7	42.2	17.3	22.2	19.5	50.7	16.3	48.5	16.7	48.1	16.5	44.4	17.0
RUBi	9.9	9.0	10.1	9.8	10.0	11.4	9.8	10.2	10.0	12.3	9.7	10.9	9.9	9.2	10.1
LNL	10.4	22.4	9.6	12.1	10.8	13.5	10.6	11.3	10.9	11.5	10.8	30.8	8.6	24.8	9.3
IRMv1	24.8	52.6	21.8	58.3	21.2	26.0	24.8	57.4	21.3	53.2	21.9	53.3	21.6	49.5	22.1
$b_{expl.} = \text{Distractor Shape+Texture Pattern+Digit Color+Background Color+Texture Color+Distractor Color+Digit Position}$															
Up Wt	44.0	70.5	41.4	73.9	41.0	48.8	43.9	71.8	41.2	71.8	41.4	71.0	41.2	68.2	41.6
GDRO	16.6	42.6	13.7	34.6	14.7	19.0	16.4	46.8	13.3	46.5	13.4	44.1	13.4	38.9	14.1
RUBi	10.0	11.9	10.6	10.2	10.8	10.7	10.7	10.2	10.8	12.6	10.5	11.2	10.7	9.7	10.8
LNL	10.0	10.1	11.5	10.5	11.4	11.1	11.4	12.2	11.2	12.8	11.2	11.4	11.3	10.7	11.4
IRMv1	21.8	47.7	19.0	51.6	18.6	24.6	21.6	49.8	18.7	52.2	18.6	49.3	18.7	46.5	19.1
Implicit Methods															
LFF	56.6	71.2	55.4	82.6	54.2	63.8	56.3	77.0	54.8	74.6	55.1	76.2	54.8	75.4	54.9
SD	41.3	69.5	38.3	71.2	38.1	46.3	40.9	72.2	38.0	72.1	38.1	71.1	38.0	70.5	38.2



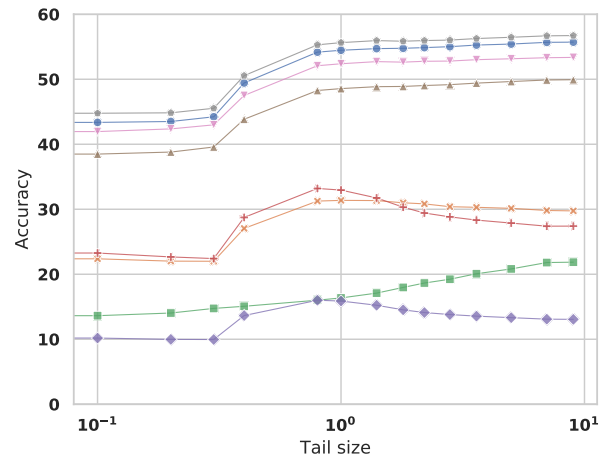
(a) Explicit Bias = Head vs Tail (# groups = 2)



(b) Explicit Bias = Global Group (# groups = 115)



(c) Explicit Bias = Answer Class (# groups = 1833)



(d) Explicit Bias = Local Group (# groups = 133,328)



Figure A9: Tail accuracies on GQA-OOD, when considering 4 different explicit biases.

Table A6: Hyperparameters for all datasets for all the comparison methods selected using unbiased accuracies of the validation sets after performing grid search over hyperparameters.

Methods/Datasets	Parameters	CelebA	Biased MNIST	GQA-OOD
Common to all methods unless specified otherwise	Optimizer	SGD	Adam	Adam
	Batch Size	128	128	128
	Epochs	50	30	30
Standard Model (StdM)	Learning Rate	10^{-3}	10^{-3}	10^{-4}
	Weight Decay	0	10^{-5}	0
Group Upweighting (Up Wt) [56]	Learning Rate	10^{-5}	10^{-3}	10^{-3}
	Weight Decay	0.1	10^{-5}	0
Group DRO (GDRO) [55]	Learning Rate	10^{-5}	10^{-3}	10^{-4}
	Weight Decay	0.1	10^{-5}	0
	Step Size	0.01	10^{-3}	0.01
Reduction of Unimodal Biases (RUBi) [13]	Learning Rate	10^{-4}	10^{-3}	10^{-4}
	Weight Decay	10^{-5}	10^{-5}	0
Adversarial Regularization (LNL) [38]	Learning Rate	10^{-4}	10^{-3}	10^{-3}
	Weight Decay	10^{-4}	10^{-5}	0
	Gradient Reversal Weight ($\lambda_{grad.}$)	-0.1	-0.1	-0.1
	Entropy Loss Weight ($\lambda_{ent.}$)	0	0.01	0.01
Invariant Risk Minimization (IRMv1) [5]	Learning Rate	10^{-4}	10^{-3}	10^{-4}
	Weight Decay	0	10^{-5}	0
	Gradient Regularization Weight ($\lambda_{grad.}$)	1.0	0.01	0.01
	Number of environments per mini-batch	4	16	16
Learning From Failure (LFF) [46]	Optimizer	Adam	Adam	Adam
	Learning Rate	10^{-4}	10^{-3}	10^{-4}
	Weight Decay	0	10^{-5}	0
	Amplification Factor (γ)	0.1	0.5	0.7
Spectral Decoupling (SD) [50]	Learning Rate	10^{-4}	10^{-3}	10^{-4}
	Weight Decay	10^{-5}	10^{-5}	0
	Output Decay (λ)	$\lambda_0 = 10$ $\lambda_1 = 10$	10^{-3}	10^{-3}
	Output Shift (γ)	$\gamma_0 = 0.44$ $\gamma_1 = 2.5$	10^{-3}	10^{-3}

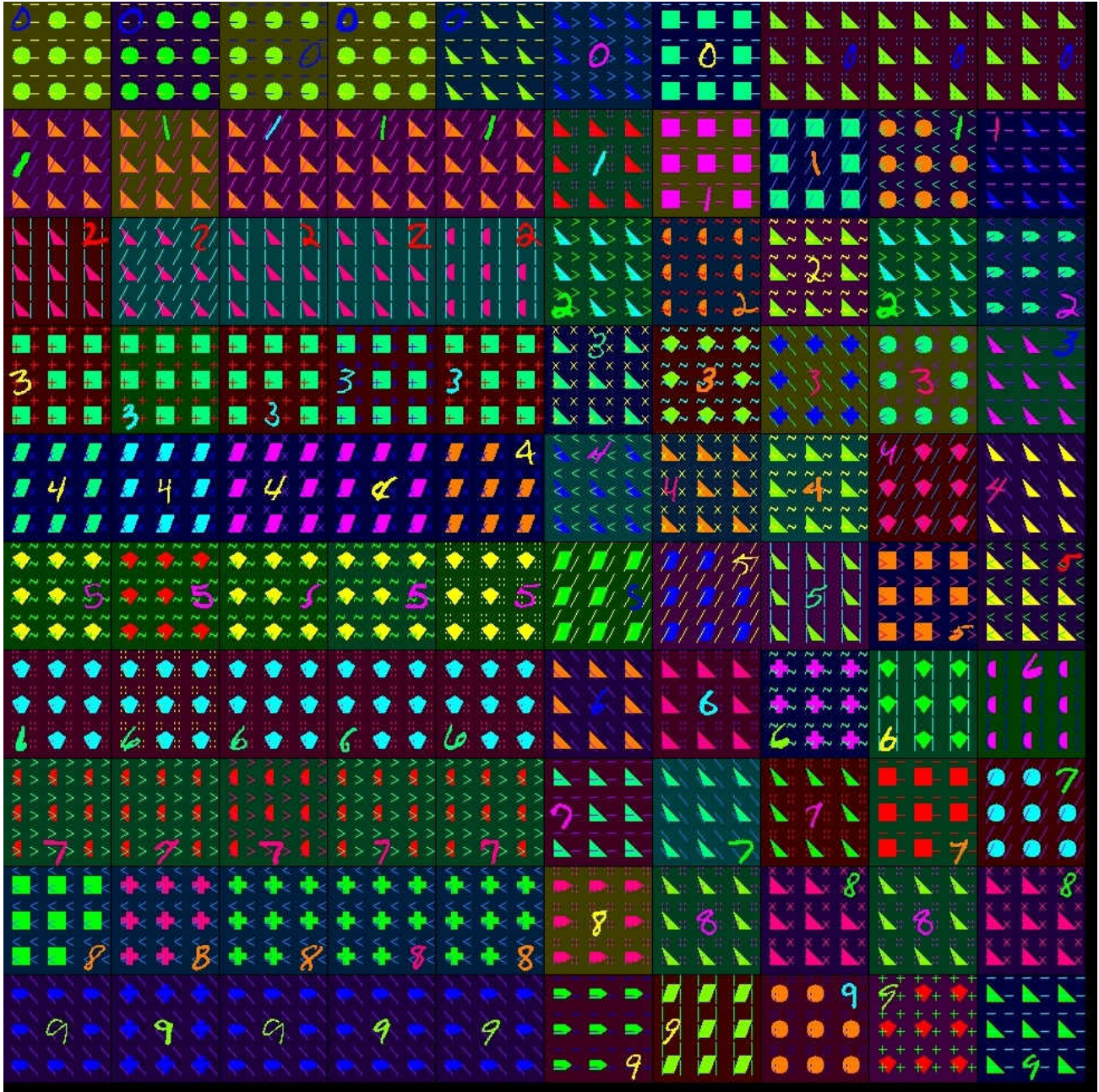


Figure A10: Biased MNIST requires the methods to classify the target digit while remaining invariant to biases.